

Operation, System Architectures, and Physical Layer Design Considerations of Distributed MAC Protocols for UWB

Nathaniel J. August, *Member, IEEE*, and Dong Sam Ha, *Senior Member, IEEE*

Abstract—Impulse-based ultra wideband (I-UWB) is an attractive radio technology for large *ad hoc* and sensor networks due to its robustness to harmful multipath effects, sub-centimeter ranging ability, simple hardware, and low radiated power. To scale to large sizes, networks often implement distributed medium access control (MAC) protocols. However, most MAC protocols for I-UWB are centralized, and they target small wireless personal area networks and cellular networks. We propose three distributed MAC protocols suitable for I-UWB. Two multichannel protocols, called multichannel pulse sense multiple access (M-PSMA) and multichannel ALOHA achieve high aggregate throughput. A busy-signal protocol, called busy-signal multiple access (BSMA), reduces the energy wasted from re-transmitted packets. This paper describes the three protocols in terms of the protocol's operation, the supporting system architecture, and the I-UWB physical layer. Physical layer simulations confirm the feasibility of implementing the proposed systems and also provide parameters for network simulations. Network simulations show that the throughput of M-PSMA exceeds that of a centralized time-division multiple-access protocol and that the energy efficiency of BSMA far surpasses that of other distributed protocols.

Index Terms—*Ad hoc* and sensor networks, busy-signal multiple access (BSMA), medium access control (MAC), pulse sense, ultra-wideband (UWB).

I. INTRODUCTION

IMPULSE-BASED ultra-wideband (I-UWB) is an attractive radio technology for *ad hoc* and sensor networks due to its low radiated power, robustness to harmful multipath effects, sub-centimeter ranging ability, and simple hardware [1]–[4]. Most medium access control (MAC) protocols for I-UWB are centralized, and they target small wireless personal area networks (WPANs) and cellular networks [5]–[18]. For *ad hoc* and sensor networks with a large number of nodes, these protocols impose impractical constraints such as central coordination (which leads to a central point of failure), more complex hardware, or control traffic overhead.

Manuscript received January 2, 2006; revised March 8, 2006.

N. J. August was with the Very Large Scale Integration for Telecommunications Laboratory, Bradley Department of Electrical and Computer Engineering, Virginia Polytechnic Institute and State University, Blacksburg, VA 24061 USA. He is now with the Intel Corporation, Portland, OR 97124 USA (e-mail: nate_august@yahoo.com).

D. S. Ha is with the Very Large Scale Integration for Telecommunications Laboratory, Bradley Department of Electrical and Computer Engineering, Virginia Polytechnic Institute and State University, Blacksburg, VA 24061 USA (e-mail: ha@vt.edu).

Digital Object Identifier 10.1109/TMTT.2006.877424

To scale to a large size, networks generally implement distributed MAC protocols because distributed protocols do not complicate hardware, require central coordination, or add control traffic overhead [19]–[23]. In a previous study [24], we characterized the network performance of distributed MAC protocols suitable for I-UWB. In this paper, we further analyze the operation of three MAC protocols and describe the supporting system architectures. In addition, this paper presents simulations that reflect physical layer considerations such as channel effects. These physical layer simulations confirm the feasibility of implementing the proposed systems and also provide parameters for network simulations.

Two of the proposed protocols are classified as multichannel protocols and the third is classified as a busy-signal protocol.

First, we explore the two multichannel protocols: multichannel ALOHA (M-ALOHA) and multichannel pulse sense multiple access (M-PSMA). Each sub-channel in M-PSMA and M-ALOHA operates at the full channel data rate, whereas each sub-channel in a traditional multichannel protocol operates at a fraction of the full channel data rate. An optional multiuser receiver, which can receive on multiple sub-channels simultaneously, further improves performance with moderate additional hardware complexity.

Next, we investigate the busy-signal protocol, i.e., busy-signal multiple access (BSMA). BSMA improves energy efficiency by decreasing the number of collisions and also by reducing the energy wasted on the collisions that do occur. Whereas narrowband systems require two transceivers to implement a busy-tone MAC, the proposed I-UWB system requires only a single transceiver to save cost, power, and circuit complexity.

This paper is organized as follows. Section II reviews I-UWB signaling, our base transceiver architecture, and related work by others on MAC protocols. Section III focuses on the multichannel protocols M-PSMA and M-ALOHA, while Section IV concentrates on the busy-signal protocol BSMA. Sections III and IV explain the operation, system architecture, and physical layer considerations for the proposed protocols. Sections III and Section IV also present physical layer simulation results. Section V presents network simulation results, and Section VI concludes this paper.

II. PRELIMINARIES

A. I-UWB Signaling

An I-UWB signal consists of a series of sharp pulses with duration of a few hundred picoseconds to a few nanoseconds.

The pulses repeat at a pulse repetition interval (PRI) that ranges from nanoseconds to microseconds. Our proposed MAC protocols benefit from I-UWB signals with a PRI in the approximate range from 1 μ s to 10 ns. We claim that PRIs in this range are *moderate*, as described below.

For PRIs shorter than our moderate range, systems must overcome several challenges. One challenge is that the channel delay spread starts to become longer than the PRI so an I-UWB communications system encounters significant inter-symbol interference (ISI). Another challenge is that, as pulses appear more frequently, each pulse must decrease in energy to meet the Federal Communications Commission (FCC)'s average (over many PRIs) power limits of -41.3 dBm/MHz [25]. In addition, the amplitude of spectral lines relative to the average power increases with decreasing PRI. Thus, a system designer cannot arbitrarily decrease the PRI to improve throughput without some cost.

For PRIs longer than our moderate range, the pulse repetition frequency (PRF) ($PRF = 1/PRI$) approaches the bandwidth of narrowband victim receivers. The FCC regulates the peak power of a single pulse¹ to prevent overloading nearby narrowband victim receivers. Thus, a system designer cannot arbitrarily increase the PRI to improve the signal-to-noise ratio (SNR).

B. Base I-UWB Transceiver

Our base I-UWB transceiver targets CMOS implementation because the low power dissipation and low cost are suited to *ad hoc* and sensor networks. All the critical front-end transceiver components have been fabricated and tested in a 0.18- μ m CMOS process [26]–[29]. The fabricated components include a power amplifier (PA), variable gain amplifiers, peak detectors, a low-noise amplifier (LNA), a phase-locked loop, an analog-to-digital converter, the filters, and a transmit/receive (T/R) mechanism. Instead of using a typical T/R switch, our system toggles the disable inputs to the PA and LNA. This scheme improves the switching time to 250 ps (which is much faster than our fastest PRI of 10 ns), and it avoids the additional noise and insertion loss of a T/R switch. A pulse sensor unit quickly and reliably detects I-UWB traffic just as carrier sense detects narrowband signals [30]. The pulse sensor's analog components occupy less than 3% of the total transceiver area, and its digital circuitry requires a few hundred transistors. The remaining design work consists of digital blocks for baseband signal processing and for implementing our proposed MAC protocols.

System-level simulations and CMOS measurements of the transceiver show that the performance is more than adequate for *ad hoc* and sensor networks at moderate pulse rates. The transceiver achieves a bit error rate (BER) of approximately 2×10^{-4} for a link distance of 10 m in extreme nonline-of-sight (NLOS) channel conditions at a data rate of 100 Mb/s without channel coding [31], [32]. Lowering the data rate (via spreading or reducing the pulse rate to around 50 ns, where FCC regulations begin to limit peak power) can increase the link distance or improve the BER. The transceiver dissipates an estimated 600 μ W of power when actively transmitting and 180 mW when actively receiving. Low power design techniques, such as reduced ADC

¹The peak power limit is $20 \log$ (RBW/50 MHz), where "RBW" denotes the victim receiver bandwidth centered on the frequency of peak UWB power [23].

resolution or sleep modes, can significantly reduce the average power from the active power levels [33].

Although the complete transceiver is not integrated in a single chip, we believe that the fabrication and testing of the front-end components and the simulations of the system show that there are no significant barriers to implementing an integrated system.

C. MAC Protocols

Most MAC protocols for I-UWB are centralized, and they target small WPANs and cellular networks [5]–[18]. A central controller assigns concurrent transmissions to multiple sub-channels via time division multiple access (TDMA) [9], [10], time-hopping codes [5]–[8], frequency-hopping codes [11]–[14], or direct sequence codes [15]–[18]. Such centralized multichannel approaches are a good strategy for small networks with heavy traffic and strict quality of service (QoS) requirements. However, in large *ad hoc* and sensor networks, the centralized control does not scale well. Control traffic significantly increases the amount of overhead, thus wasting bandwidth and energy. Further, because nodes may not be easily serviceable (e.g., battlefields), a central failure would render the network useless.

Some multichannel protocols are modified to distributively determine a transmission's sub-channel based on the address of the receiver [34] or the sender [35]. However, to prevent simultaneous transmissions to one node, these protocols incur overhead to establish a link [34], [35] and may require techniques such as adaptive coding to mitigate strong multiuser interference [34]. Design guidelines for distributed multichannel protocols are suggested in [36]. In addition to controlling medium access, a distributed management system may also control QoS [37].

Instead of altering existing I-UWB protocols to become more distributed, we propose fundamentally distributed approaches to scale to large *ad hoc* and sensor networks. In a distributed protocol, each node independently decides to transmit without central guidance. This reduces control overhead, and there is no central synchronization or central point of failure. However, as described below, adoption of some existing distributed MAC protocols is impractical for I-UWB [19]–[23].

ALOHA is a basic distributed MAC protocol that can be applied to I-UWB in a straightforward manner. In ALOHA, a node may transmit a data packet anytime, unless it is busy with another packet. If the data transmission succeeds, the target node responds with an acknowledgment (ACK) packet. Otherwise, the source node waits a random period of time to retransmit the data. ALOHA performs well under light traffic, but poorly under heavy traffic.

In narrowband systems, carrier sense multiple access (CSMA) improves on ALOHA by requiring a node to check for a busy medium before transmitting [19]–[21]. For I-UWB, a pulse sensor enables an analogous protocol, i.e., pulse sense multiple access (PSMA) [30]. However, hidden terminal conditions cause poor performance in CSMA and PSMA.

Narrowband systems mitigate hidden terminal conditions via collision avoidance (CA) with time-duplexed request-to-send (RTS) and clear-to-send (CTS) packets. For I-UWB, the RTS and CTS packets add excessive overhead in PSMA with CA

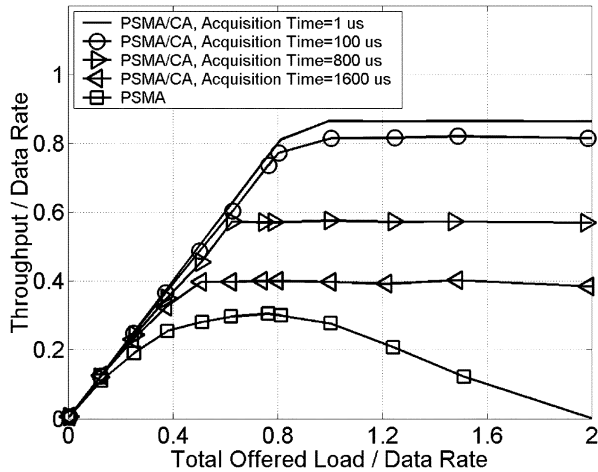


Fig. 1. Throughput for PSMA, PSMA/CA as acquisition time increases. The transmitting nodes are hidden from one another.

(PSMA/CA) [20], [38]. The narrow pulses, low radiated power, harsh channel conditions, and strict FCC power limits combine to produce long acquisition times, which results in excessively long preambles for the RTS and CTS packets.

Fig. 1 shows the shortcomings of PSMA and PSMA/CA in a linear network of three I-UWB nodes A–B–C. Nodes A and C are hidden from one another, and they both transmit to B with a 1-Mb/s data rate. The time between packets follows a Poisson distribution such that nodes A and C transmit at an average of $0.5 \times \text{offered load}$. Using serial correlation, practical acquisition times for I-UWB range from 800 to 1600 μs (800 to 1600 symbols), compared to approximately 100 μs for a narrowband system. Such long acquisition times significantly degrade the throughput for PSMA/CA due to the overhead of the RTS and CTS packets. PSMA performs poorly due to the hidden terminal condition. Our proposed MAC protocols exploit the unique signaling of I-UWB to improve performance over PSMA and PSMA/CA.

III. MULTICHANNEL MAC PROTOCOLS FOR I-UWB SYSTEMS

Multichannel MAC protocols are known to reduce collisions without the overhead of RTS and CTS packets [22]. A multichannel MAC protocol divides a channel of bandwidth W into Y sub-channels of bandwidth W/N , where N is the spreading factor or number of time slots. Note that Y is not necessarily equal to N , especially in code division. Although multichannel protocols reduce the link data rate by a factor of N , they increase overall network throughput at high offered load. A node may select from a greater number of (ideally) orthogonal sub-channels so there is a smaller probability of collisions. However, the reduced data rate of each sub-channel incurs a delay penalty at low offered load.

A. Operation of M-ALOHA and M-PSMA

We propose two distributed multichannel MAC protocols, called M-ALOHA and M-PSMA, that exploit the inherently low duty cycle of I-UWB to implement sub-channels. Depending

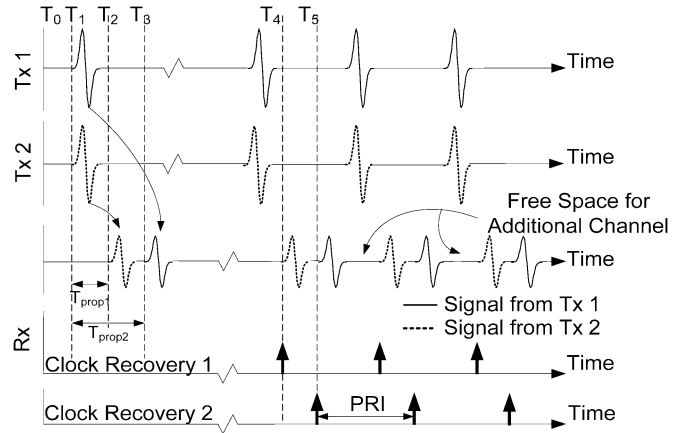


Fig. 2. Multichannel MAC operation [24].

on the pulse rate and channel conditions, I-UWB signals may contain a large amount of “dead time” between pulses. This dead time is used to time-interleave additional sub-channels. Each sub-channel maintains the full data rate, so the network increases throughput without increasing delay.

In M-PSMA, nodes may transmit any time they sense an idle channel. If a node senses activity, it waits until after the medium is free to retransmit. A source node also waits for a random period of time to retransmit if it does not receive an acknowledgement. The random time period is bounded by a binary exponential. The operation of M-ALOHA is similar, but it does not check for an idle channel before transmitting.

The M-PSMA and M-ALOHA protocols provide multiple time-interleaved channels by allowing concurrent transmissions of nonoverlapping pulse trains. During an initial reception, the receiver may acquire (for a multiuser receiver) or ignore (for a single-user receiver) other concurrent nonoverlapping transmissions. For example, in Fig. 2, two nodes sense an idle channel at time T_0 so they simultaneously start transmitting at time T_1 to the same receiver. The receiver detects an incoming transmission through the pulse sensor. Transmitter 2 is closer, so its first pulse arrives at time T_2 , while Transmitter 1’s first pulse arrives at T_3 . After some time, a single acquisition circuit detects the arrival time of the two pulse trains within a PRI. If the receiver is a multiuser receiver, two clock recovery circuits track Transmitter 2’s pulse train starting at T_4 and Transmitter 1’s pulse train starting at T_5 . The receiver time-shares a single demodulator between the incoming signals. If the transmissions target different nodes, the receiver would track and decode only its own transmission. If the receiver is single user, it would track only Transmitter 2’s pulse train and ignore Transmitter 1’s pulse train because Transmitter 2’s pulse train precedes Transmitter 1’s.

If two or more nodes transmit simultaneously, a collision can occur only if the pulses (including multipaths) overlap within a PRI. To quantify this, consider a version of M-ALOHA that allows up to D sub-slots² per PRI, so there may be maximum of D simultaneous transmissions that do not share any common

²We use the term “sub-slot” to denote the number of multipath-delay-spread-sized time units within a PRI. This is to differentiate a sub-slot from a slot, which often denotes a packet-sized unit of time in a slotted MAC protocol.

sub-slots. For X nodes transmitting, the probability P_S that two or more nodes share a slot is

$$P_S = \begin{cases} 1 - \frac{D!}{((D-X)!D^X)}, & X \leq D \\ 1, & X > D. \end{cases} \quad (1)$$

We now consider the performance of a system with $D = 40$ slots because a long multipath delay spread is 25 ns [39], a 1-Mp/s pulse rate has a PRI of 1000 ns, and $1000/25 = 40$. From (1), it is improbable ($P_S = 0.025$) that two concurrent transmissions ($X = 2$) overlap in time at a single receiver. P_S gradually approaches 100% as X increases to D , but it also becomes increasingly improbable that many more than two nodes transmit concurrently because the number of possible interfering transmissions is limited by the number of neighbors. To ensure a connected topology in large networks with power control, note that the critical number of neighbors is approximately $\ln z$, where z is the total number of nodes [40].

The probability that X neighbor nodes transmit during a packet time is designated $P_T = P(X \text{ nodes transmit})$, and this probability depends on the application. For illustrative purposes, we assume the nodes transmit with a Poisson distribution at a mean rate of G packets per packet time. Since the number of nodes transmitting is independent of the time of transmission within a PRI, P_T and P_S are independent. The probabilities of collision for the proposed M-ALOHA protocol and for a single-channel protocol are

$$P_C^{\text{multichannel}} = \sum_{X>1} P_T \times P_S \quad (2)$$

$$P_C^{\text{single channel}} = \sum_{X>1} P_T. \quad (3)$$

For X such that $2 \leq X \leq D$, $P_C^{\text{multichannel}}$ must be less than $P_C^{\text{single channel}}$ because $0 < P_S < 1$. This decreased probability of collision is a huge benefit compared to a single-channel protocol in which the probability of collision is 100% if two or more nodes transmit simultaneously.

For the proposed multichannel I-UWB protocols, the probability of a collision remains low even when G is greater than the number of packets per packet time, i.e., the protocol can offer a throughput *larger* than the aggregate data rate. For example, with $G = 3.0$, the above M-ALOHA protocol has a 90% ($1 - P_C^{\text{multichannel}}$) chance of a successful transmission, whereas a single channel protocol has only a 20% ($1 - P_C^{\text{single channel}}$) chance of success. Thus, M-ALOHA and M-PSMA can mitigate the reduction in throughput caused by collisions without the overhead of handshaking packets.

B. System Architecture

For each sub-channel, the receiver in Section II (in either a single-user or multiuser configuration) collects signal energy over a time window $T_0 = 3$ ns around the strongest multipath cluster from the signal of interest. The receiver can resolve a single signal within T_0 so 3 ns is also the minimum sub-slot time.

Multiuser receivers, which can receive on several sub-channels concurrently, improve performance over a single channel

receiver [22]. However, traditional multiuser receivers are unsuitable for large *ad hoc* and sensor networks. A receiver under a TDMA protocol is inherently multiuser, but it requires centralized control. A multiuser receiver under a code-division protocol requires separate correlators for each sub-channel, and a multiuser receiver under a frequency-division protocol requires a separate front-end for each channel.

Under M-PSMA and M-ALOHA, an I-UWB system can implement a multiuser receiver with simpler hardware and no central control [41]. Each supported sub-channel requires only a dedicated clock recovery circuit. If the receiver detects more than one incoming transmission during acquisition, it assigns an available clock recovery circuit to each nonoverlapping incoming transmission. After acquisition, the acquisition circuit continues to look for nonoverlapping transmissions. Since the resolvable transmissions do not overlap, they may time-share a single front end and a single decision block.

C. Physical Layer Design Considerations

When the pulses from two interleaved pulse trains appear close in time to each other, the multipath spread from the first pulse interferes with the second. The effective interference is determined by the delay between the pulses, the signal to interfering signal (S/I) level, the channel power delay profile, and the channel delay spread. The receiver must separate the intended signal from the received signal $r(t)$ in (4) as follows:

$$r(t) = \sum_{i \in I} s_i(t - t_i) * h_i(t) + \sum_{j \in J} s_j(t - t_j) * h_j(t) + \sum_{k \in K} s_k(t - t_k) * h_k(t) + n(t) \quad (4)$$

where

- $s_i(t)$ data signal from a node $i \in I$, the set of all nodes whose transmissions experience a collision;
- $s_j(t)$ data signal from a node $j \in J$, the set of all nodes whose transmissions experience interference, but not a collision;
- $s_k(t)$ data signal from a node $k \in K$, the set of all nodes whose transmissions do not experience interference or a collision;
- t_i , time offset of arrival within a PRI of signal from node i . $\forall i \in I, \exists n$ s.t. $(t_j - t_n) \leq T_0$ for $i \neq n$ and receiver time window T_0 ;
- t_j time offset of arrival within a PRI of signal from node j . $\forall j \in J, \exists n$ s.t. $(t_j - t_n) \leq D$ for $j \neq n$; also, $\forall j, n, T_0 < (t_j - t_n)$ for $j \neq n$, where D is the multipath delay spread;
- t_k time offset of arrival within a PRI of signal from node k . $\forall k, n, D < (t_k - t_n)$ for $k \neq n$;
- $h_i(t)$ channel response from node i to the receiver;
- $h_j(t)$ channel response from node j to the receiver;
- $h_k(t)$ channel response from node k to the receiver;
- $n(t)$ noise at the receiver.

As implied by (4), nodes can be broken into the three groups I , J , and K . First, consider the case with a received transmission

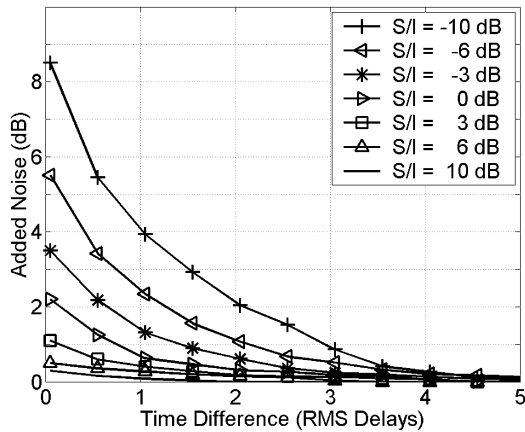


Fig. 3. Interference from overlapping transmissions.

from node $i \in \mathbf{I}$. Since the receiver in Section II cannot differentiate between signals that arrive within one time window T_0 of each other, it discards all transmissions from nodes in group \mathbf{I} , and they are considered as collisions.

Using physical layer simulations in Agilent's Advanced Design System (ADS), we characterize the interference from a node n to a node $m \in \mathbf{J}$ or \mathbf{K} . The simulations use binary phase-shift keying (BPSK) modulation, and the second arriving pulse is 6 dB over the receiver's minimum sensitivity level. The power level of $s_n(t)$ results in S/I levels from -10 dB to $+10$ dB to encompass a 10-m radius. Although an S/I level of $+10$ dB places the average interference power below the sensitivity level, the instantaneous power may affect reception. We also vary the delay ($t_m - t_n$) between the pulses. We start with a delay of T_0 (3 ns) and stop when $s_n(t)$ no longer interferes with $s_m(t)$. Fig. 3 shows simulation results from an average of 20 random implementations of the IEEE 802.15.3a channel model CM4 [39]. As expected, the interference decreases as the delay between pulses increases and as the S/I ratio increases.

For a node $j \in \mathbf{J}$, the pulses arrive at the receiver at least one time window later than a pulse from node n , and multipaths from $s_n(t)$ interfere with $s_j(t)$. For example, with an S/I of -10 dB, Fig. 3 shows that $s_n(t)$ adds an average of approximately 8.5 dB of noise to $s_j(t)$ when the time difference is T_0 and an average of 2 dB of noise when the time difference is two rms delay spreads.

For a node $k \in \mathbf{K}$, multipaths from $s_n(t)$ do not significantly interfere with $s_k(t)$. We consider a transmission to be from a node in \mathbf{K} if it experiences an effective noise level less than a cutoff of 0.1 dB. For an S/I of -10 dB, Fig. 3 shows that this occurs around a time difference of five rms delay spreads.

Results similar to Fig. 3 characterize the interference among transmissions for the network simulations in Section V. Instead of using an average, each link has a unique channel model. The added noise is obtained for each pair-wise set of transmissions from lookup tables indexed by the S/I ratio, the channel model, and the time difference between pulses.

IV. BUSY-SIGNAL MAC PROTOCOL FOR I-UWB SYSTEMS

M-ALOHA and M-PSMA improve throughput, but collisions still waste energy by forcing nodes to retransmit entire packets.

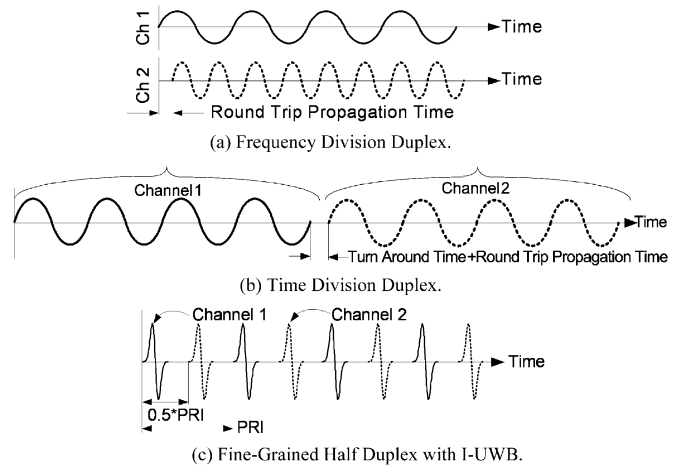


Fig. 4. Types of duplexing [45].

Collision detection or CA could reduce the wasted energy. However, collision detection normally requires an additional transceiver to duplex feedback signals in a frequency band separate from the data. From Section II, CA adds excessive overhead in I-UWB. An energy-efficient busy-signal MAC protocol, called BSMA, that avoids the hardware cost of collision detection and the overhead of CA is proposed here.

A busy signal provides three important services to the MAC layer, which are: 1) preventing nodes within range of the destination from initiating a transmission; 2) informing the source node of a successful transmission; and 3) requesting the source node to terminate transmission of a corrupt packet so it does not waste energy transmitting the entire packet. The busy signal effectively acts as a symbol-level ACK. BSMA may require a busy signal to be emitted by any node that detects a transmission [42], or by the destination node only [43]; or first, by any node that detects a transmission and then, by only the destination node after address decoding is complete [23]. Our implementation follows that in [23].

A. Duplexing

To implement a busy signal, a transceiver must be capable of full duplex operation [44]. Narrowband radios implement full duplex operation with frequency division duplexing (FDD), which requires two transceivers in different frequency bands. The FDD system in Fig. 4(a) can transmit a busy signal and receive a data signal simultaneously, but the additional frequency band is inefficient in hardware complexity, power dissipation, and spectral usage.

Since FDD is expensive, narrowband systems usually implement time-domain duplexing (TDD), as shown in Fig. 4(b). CA protocols use TDD, and the acquisition overhead for each time-duplexed packet incurs penalties in throughput, energy efficiency, and latency. Further, a TDD system cannot detect a packet error until after the transaction completes, thus it wastes energy transmitting corrupted data. TDD is especially unattractive for energy-sensitive networks operating in harsh channel conditions

We propose a fine-grained half duplex for I-UWB that achieves full duplex performance with a single transceiver.

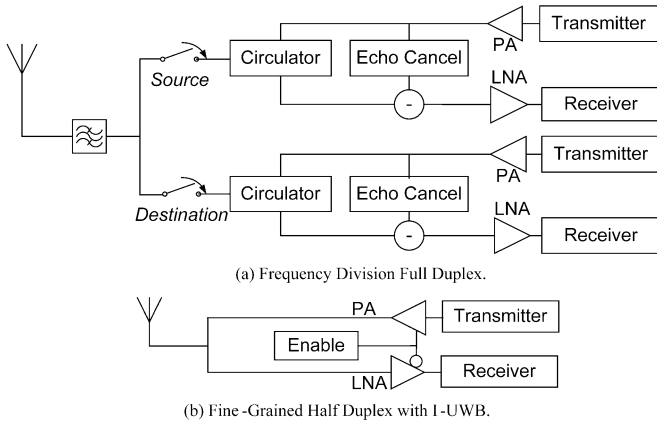


Fig. 5. Full duplex system architectures [24].

An I-UWB signal is not continuous in time like a narrowband signal, thus the idle time between data pulses can serve as a feedback channel for a busy signal. The I-UWB system in Fig. 4(c) achieves full duplex performance without the energy, latency, and throughput penalty of the TDD system and without the additional frequency band of the FDD system. Starting in receive mode, a transceiver receives a data pulse. It then switches to transmit mode and transmits a busy-signal pulse. After transmitting, it switches to receive mode and prepares for the next data pulse. The fine-grained half duplex switches between receive and transmit modes on a symbol level, but it appears as full duplex at the MAC level.

B. System Architecture

Fig. 5 compares an FDD architecture for narrowband radios to the proposed fine-grained half duplex architecture for I-UWB radios. An *ad hoc* network has no base station to translate between frequency bands for inter-node communication. Therefore, the narrowband radio in Fig. 5(a) must be capable of operating in either band, depending upon whether it is a source or destination node. The dual bands result in a radio, with two transceivers and two circulators, that demands more than twice the power and hardware cost of a single transceiver. The feedback channel also degrades spectral efficiency.

With the proposed I-UWB system in Fig. 5(b), the low duty cycle allows a single transceiver to access a feedback channel in the same frequency band as the transmitted data. Since the data signal and the busy signal share a band, they also share RF circuitry. The switching time between transmit and receive modes determines the minimum PRI. The receiver in Section II toggles the disable inputs to the PA and the LNA to achieve a switching time of 250 ps, which is much faster than our fastest PRI of 10 ns. The proposed I-UWB transceiver significantly reduces circuit cost and power dissipation as compared to a narrowband FDD transceiver. Further, the system leverages the low transmit power of I-UWB by transmitting a busy signal for the duration of a successful transaction, while only periodically checking for a busy signal.

C. Physical Layer Design Considerations

A node q under BSMA can be a source node, a destination node, or an idle node. The busy signal should not degrade data reception at a destination node, and it should be easily detectable by a source node or an idle node with data to transmit. Interference complicates these goals. After the destination node transmits a busy signal, the multipath channel causes a long ring down time, and some of the busy-signal multipaths could interfere with data reception. Likewise, the source node's data signal may interfere with busy-signal detection. When multiple nodes emit busy signals, they may interfere with both data reception and busy-signal detection. The received signal $r_q(t)$ for a node q is given in (5) as follows:

$$r_q(t) = x_{\text{LNA}}(t) * \left[x_{\text{PA}}(t) * s_q(t - t_d) + \hat{s}_p(t - t_{p,q}) * h_{p,q}(t) + n(t) + \sum_{v \in V} d_v(t - t_{v,q}) * h_{v,q}(t) + \sum_{u \in U} b_u(t - t_{u,q}) * h_{u,q}(t) \right] \quad (5)$$

where

$x_{\text{PA}}(t)$	impulse response of the PA in state $w \in [\text{on}, \text{off}]$;
$x_{\text{LNA}}(t)$	impulse response of the LNA in state $\hat{w} \in [\text{off}, \text{on}]$;
$s_q(t)$	signal transmitted by node q (data or busy signal);
$\hat{s}_p(t)$	signal received by node q from its link partner, node p ;
$b_u(t)$	signal from a node $u \in U$, the set of all nodes $\neq p$ transmitting a busy signal, including q if it is a destination;
$d_v(t)$	signal from a node $v \in V$, the set of all nodes $\neq p$ transmitting a data signal, including q if it is a source;
$h_{x,q}(t)$	channel impulse response of any node x to node q ;
$t_{x,q}$	propagation delay from any node x to node q ;
t_d	internal delay from the transmitter to the receiver;
$n(t)$	the receiver noise at node q .

A node should mitigate the strong interference from its own transmission $s_q(t)$ such that ideally

$$\int x_{\text{LNA}}(t) * x_{\text{PA}}(t) * s_q(t - t_d) dt = 0. \quad (6)$$

Since the switching time is not instantaneous, we enable/disable the PA/LNA such that either w or \hat{w} is always off. Thus, to prevent interference from $s_q(t)$, the timing sequence consists of 0.25 ns for the transition $[\hat{w} = \text{on} \rightarrow \hat{w} = \text{off}]$, 0.25 ns for the transition $[w = \text{off} \rightarrow w = \text{on}]$, the transmitted pulsewidth time (usually less than 1 ns), 0.25 ns for the transition $[w = \text{on} \rightarrow w = \text{off}]$, and 0.25 ns for the transition $[\hat{w} = \text{off} \rightarrow \hat{w} = \text{on}]$.

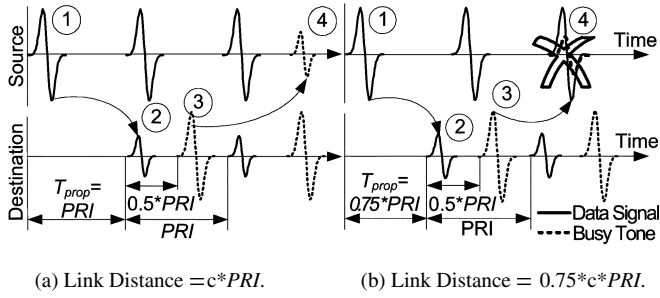


Fig. 6. Overlap effect at source node [45].

Next, a node should separate $\hat{s}_p(t)$ from other data and busy signals and from its own reflected multipaths such that ideally

$$\int \left[\sum_{u \neq p} b_u(t - t_{u,q}) * h_{u,q}(t) + \sum_{v \neq p} d_v(t - t_{v,q}) * h_{v,q}(t) \right] * \hat{s}_p(t - t_{p,q}) * h_{p,q}(t) dt = 0. \quad (7)$$

To mitigate the interference in (7), we separate the data signal from the busy signal. Spreading the busy signal, as in direct-sequence ultra-wideband (DS-UWB), differentiates the busy signal from the data signal [17]. To prevent multiple busy signals from combining destructively, the DS-UWB code minimizes autocorrelation. Orthogonal pulse shapes also separate the busy signal from the data signal. Finally, node q estimates and equalizes the reflections from its own transmitted signal. Such equalization is relatively simple because the signal is known.

The phenomenon of *overlap* may also degrade performance [44], [45]. Depending on the link distance, a busy-signal pulse may overlap a data pulse in time at either the source node or destination node. For clarity, we allow the destination to time its busy-signal transmission to avoid any overlap with the received data signal. Thus, a source node may lose a portion of the busy signal when it transmits a data pulse with its PA enabled ($w = \text{on}$) and its LNA disabled ($\hat{w} = \text{off}$). Fig. 6 illustrates overlap at a source node. At Time 1, the source node transmits a pulse, which arrives one propagation time T_{prop} , later at the destination node at Time 2. At Time 3, the destination sends a busy-signal pulse exactly $0.5 \cdot \text{PRI}$ s after the arrival of the first data pulse. Finally, at Time 4, the source node receives the busy-signal pulse. In Fig. 6(a), the link distance is $c \cdot \text{PRI}$ m so the round-trip propagation time is $2 \cdot \text{PRI}$ s. Therefore, the busy-signal pulse arrives $2.5 \cdot \text{PRI}$ s after the corresponding data pulse. In Fig. 6(b), the link distance is $0.75 \cdot c \cdot \text{PRI}$ m, the round-trip propagation time is $1.5 \cdot \text{PRI}$ s, and the busy-signal pulse arrives $2 \cdot \text{PRI}$ s after the corresponding data pulse. Since the source node is transmitting, it loses energy from the busy signal. Note that Fig. 6 shows only the first multipath of a busy signal; in reality, a receiver could detect some portion of the multipath energy.

A source node should mitigate overlap such that ideally

$$\int x_{\text{LNA}}(t) * \hat{s}_p(t - t_{p,q}) * h_{p,q}(t) dt = \int \hat{s}_p(t - t_{p,q}) * h_{p,q}(t) dt. \quad (8)$$

To completely avoid overlap, both the source and destination nodes may wait for the maximum multipath delay spread of $D_{\text{multipath}}$ between receiving a busy-signal (data) pulse and transmitting a data (busy signal) pulse. Thus, for a maximum link distance of R_{max} , a PRI can satisfy (8) if [45]

$$\text{PRI} \geq 2 \cdot \left(\frac{R_{\text{max}}}{c} + D_{\text{multipath}} \right). \quad (9)$$

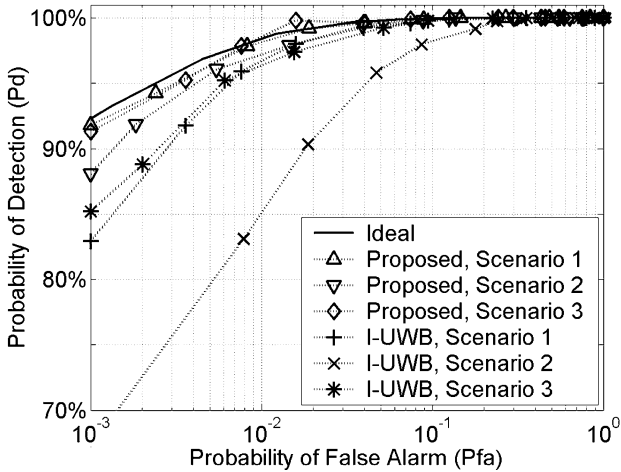
At shorter PRIs, the source node may lose up to 2 ns of the busy-signal energy from overlap and from the enable/disable timing resulting from (6). The DS-UWB scheme reduces the energy loss by spreading the busy-signal energy over a longer time period. Further, the energy from multipath reflections is available over a much longer period than 2 ns.

To mitigate the interference in (7), we have suggested three techniques, which are: 1) separating the busy signal from the data signal via DS-UWB and orthogonal pulse shapes; 2) minimizing destructive busy-signal interference by using a spreading code with low autocorrelation; and 3) equalizing self-interference. Fig. 7 compares the simulated performance of our proposed techniques (labeled *Proposed*) to a baseline I-UWB busy signal with none of the techniques (labeled *I-UWB*) and to an ideal case with no interference or overlap. The figure considers three interference scenarios. In the first, there is no overlap and a single busy signal. In the second, there is a single busy signal, and the strongest busy-signal multipaths overlap the data signal. In the third scenario, six busy signals may encounter overlap and are further corrupted by the data signal multipaths.

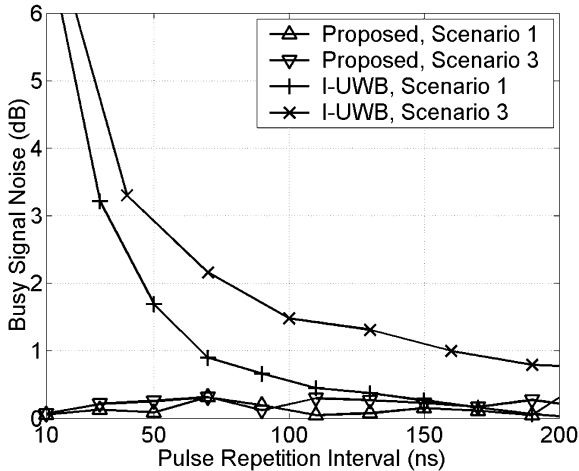
Fig. 7(a) shows the performance from the perspective of the source node. We simulate the probability of detection versus the probability of false alarm for a busy signal arriving at the source node with 3 dB less power than the data signal reflections. The destination limits its power so the strongest received busy signal has an SNR of 4 dB after an 11-dB noise figure at the antenna terminals. This SNR corresponds to a 10-m link distance at 100 Mb/s under FCC limits. The SNR is purposefully low to better compare the relative performance of the proposed methods to the ideal case. Actual systems can achieve significantly better absolute performance with multiple looks, lower data rates, or shorter link distances.

The proposed techniques improve performance for all three scenarios as compared to the baseline I-UWB case. Without overlap, equalization provides most of the performance gain. With overlap, the DS-UWB signal is responsible for the gain because the source node receiver loses less busy-signal energy. For multiple busy signals, the techniques result in smaller gains over the baseline I-UWB case because the source can detect any of the I-UWB busy signals. Note that one data point for Scenario 3 attains a higher probability of detection (100%) than the ideal case, and this is because the simulations require an impractical number of symbols to report any missed detections.

Fig. 7(b) shows the performance of the proposed techniques from the perspective of the destination node at different PRIs. The reflections from the busy signal result in a data signal to interference ratio of -3 dB. We consider the same scenarios as for the source node with the exception of Scenario 2 because the destination node times its transmission to avoid overlap.



(a) Probability of detection vs. the probability of false alarm for a busy signal at the source node.



(b) Noise added by a busy signal to the data signal at a destination node.

Fig. 7. Performance of the techniques proposed to mitigate interference and overlap in a busy-signal MAC protocol.

In the ideal case, the busy signal adds zero noise to the incoming data transmission. Of the proposed techniques, equalization is mostly responsible for reducing the noise, and the small amount of noise is due to 8-bit quantization. The estimation and equalization process is relatively simple because the busy signal is known. Without our techniques, a busy signal adds significant noise to the received signal at short PRIs. Further, multiple busy signals add more noise than a single busy signal because the destination node cannot control the time at which it receives the other busy signals. Without our techniques, a designer may need to considerably adjust the PRI (and, thus, the data rate) to meet link budget constraints.

We apply results similar to Fig. 7 in network simulations. Each pair-wise link obtains an interference level from lookup tables indexed by link distance, PRI, and channel instance.

V. NETWORK PERFORMANCE RESULTS

In [24], we presented basic network simulation results. Here, we incorporate the physical layer effects in Sections III and IV into the ns-2 simulation models. The results improve slightly over the worst case assumptions in [24]. We characterize the network

performance in terms of throughput, delay, and energy efficiency. The throughput is defined as sum of the rates (bits per second) of traffic the physical layer offers to the MAC layer of each destination node. The delay is defined as the average time a successful packet spends between the source MAC layer and the destination MAC layer. The energy efficiency is defined as the energy expended for a successful data packet divided by the total energy expended for all transmitted and received signals (note that [24] considered only the energy for data packets, not for all signals). These quantities are plotted against the offered load, which is defined as the sum of the rates (bits per second) of traffic that the network layer offers to the link layer over all nodes.

Twenty different random topologies are averaged to obtain the graphs for throughput, delay, and energy efficiency. For each simulation, we place 225 stationary nodes in random positions in a 75 m \times 75 m square area. Within a simulation, each node transmits 50 000 packets at power limits that result in a maximum link distance of approximately 10 m. Each topology produces a large variation of distances and S/I values over all possible links, but the results follow very similar trends.

The I-UWB physical layer and channel model are implemented as custom blocks in ns-2. The packet format is from [17] with a maximum data size of 4095 B and an acquisition period of 900 bits. The large maximum packet size allows the receiver to offset the overhead of the acquisition time. Traffic follows a Poisson distribution with a random source and destination for each packet. We use a spreading code only for the DS-UWB busy signal in Section IV, and there is no channel coding; so one data pulse represents one data bit. This allows us to focus on the performance of the proposed protocols—instead of the performance of a code—under the presence of the interference in (4) and (5).

To support an I-UWB physical layer, we alter ns-2 to allow simultaneous transmissions to coexist without immediately dropping a packet. To decide if a packet is dropped, ns-2 first ascertains the interference level. The interference is added to a link budget that has been calculated from system-level simulations [31], [32]. A node then drops a packet if the total interference exceeds the link budget including a 6-dB safety margin. The MAC protocols determine the unique interference level for each transmission from lookup tables.

All simulations use the 802.15.3a CM4 model because of the long rms delay spread (25 ns) [39]. Each pair-wise link randomly realizes a different channel model instance, and the characteristics remain constant over the duration of a packet.

The M-PSMA and M-ALOHA protocols obtain the interference level from lookup tables of physical layer simulation results similar to Fig. 3. For each transmission, the interference depends on the channel model between each pair of nodes, the time offset between pulses, and the S/I level of the interfering signal. The results of the lookup tables also place each transmission in group *I*, *J*, or *K*. Recall from Section III that the interference level is zero for transmissions in group *K* and that the receiver drops all packets in group *I*.

For BSMA, the source node determines the probability of detecting a busy signal from physical layer simulation results similar to Fig. 7(a). Lookup tables provide the probabilities for each transmission from the S/I ratio, the amount of overlap, and the channel model. If the source node does not detect the busy

signal, it terminates the transmission and re-transmits the packet later. The destination node determines the interference level in the received data signal via lookup tables indexed by the S/I ratio, PRI, and channel model. If the interference causes the transmission to exceed the link budget, the destination drops the transmission. As in M-PSMA and M-ALOHA, each pair-wise link uses a different channel model.

To focus on our proposed techniques, the simulator drops packets due to the interference in (4) and (5)—and not due to noise. Further, we do not include narrowband interference, as physical layer simulations show that typical narrowband interference does not significantly impact our receiver [31], [32].

For the RF circuit components, the energy dissipation is modeled from measurements of our CMOS test chips. For the digital computations associated with the MAC Layer, we model the energy with an average computational energy cost per bit. Note that, unlike narrowband systems, the baseband processing energy of I-UWB systems is comparable to the transmission energy. The receiver's energy dissipation includes the bias current of active devices, the startup energy of active devices, and the processing energy. The transmitter's energy dissipation includes the radiated energy in addition to the above sources.

For the simulations, our ns-2 implementations of the proposed MAC protocols are unslotted. In an actual deployment, the cost of centrally synchronizing the slots would be undesirable. In M-PSMA, PSMA/CA, and BSMA, nodes may transmit any time they sense an idle channel. In M-ALOHA, nodes may transmit at any time.

In Figs. 8–11, the throughput and offered load are normalized to the data rate of a single link. Thus, it is possible for the normalized throughput of the entire network to exceed unity—the maximum link data rate. Two conditions may cause the network throughput to exceed unity, which are: 1) spatial separation allows two simultaneous transmissions or 2) the pulses of two simultaneous transmissions under M-PSMA or M-ALOHA are separated in time within a PRI at the receiver.

First, we evaluate the throughput of M-ALOHA and M-PSMA. Fig. 8(a) varies the number of sub-channels M (the number of signals that the multiuser receiver in Section III can simultaneously decode) from $M = 1$ to $M = 16$ at 1 Mp/s. In all cases, M-PSMA achieves a higher throughput and is more stable than M-ALOHA. As a multiuser receiver supports more sub-channels, performance improves for both protocols, but reaches a limit around $M = 4$ for M-PSMA and $M = 8$ for M-ALOHA. This is because it is highly improbable for a node under M-PSMA to receive more than four simultaneous transmissions. The clear channel assessment (CCA) prevents any node within range of a transmitter from initiating a transmission so only hidden nodes may compete for the extra sub-channels of a multiuser receiver. Thus, adding more than four sub-channels in the multiuser receiver does not improve throughput for M-PSMA in our topologies. In M-ALOHA, nodes do not check the medium before transmitting. Thus, its performance reaches a limit at $M = 8$ because it is unlikely that a node receives more than eight simultaneous transmissions. (On average, less than 5% of the nodes have more than eight neighbors).

Fig. 8(b) shows that the benefits of M-PSMA and M-ALOHA diminish as the pulse rate increases. For a clearer comparison

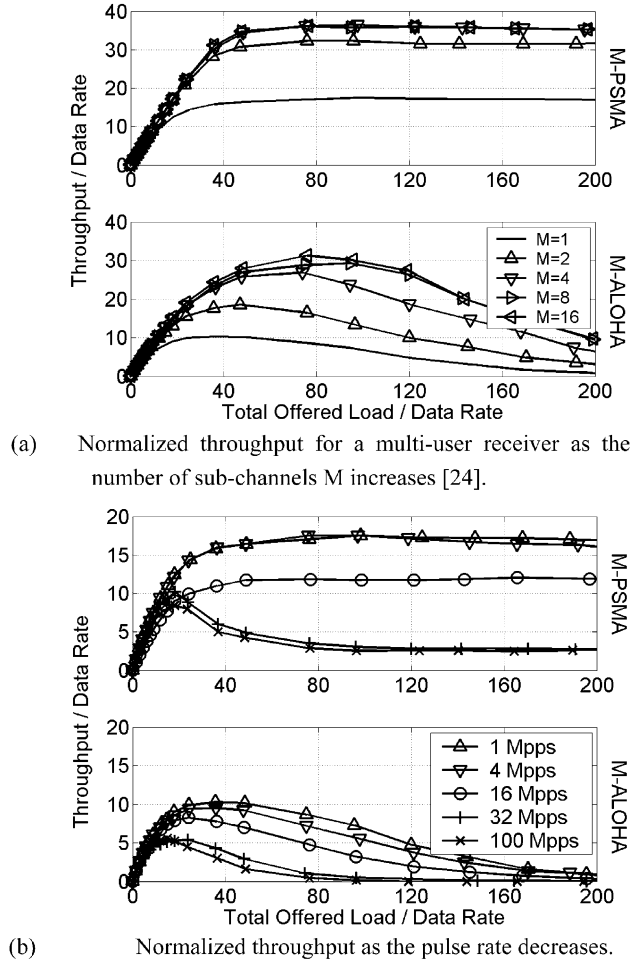


Fig. 8. Throughput for M-PSMA and M-ALOHA.

among pulse rates, the simulations assume that the hardware scales in proportion to the pulse rate. For example, at 100 Mp/s, the inter-frame times and pulse sense times are 100 times faster than at 1 Mp/s. However, the channel delay spread remains the same, thus, overlap is more probable at higher rates. The simulations consider a single-user receiver with $M = 1$ sub-channels for all pulse rates. At 1 Mp/s, the 1000 ns PRI is much longer than the rms delay spread, thus, most transmissions fall in group K . For M-PSMA, the throughput declines rapidly beyond 16 Mp/s and reaches a floor by 32 Mp/s. Beyond the throughput floor, M-PSMA operates similarly to a single-channel narrowband system, where simultaneous transmissions always overlap. This is because the PRI is on the order of the channel rms delay spread, thus, it is likely that a transmission falls in group I or J . The throughput of M-ALOHA transitions more gradually, but also reaches a floor around 32 Mp/s. Further, M-ALOHA becomes unstable at high offered loads.

Next, we evaluate the energy efficiency for M-PSMA and M-ALOHA. Fig. 9(a) varies the number of sub-channels in a multiuser receiver from $M = 1$ to $M = 16$ at 1 Mp/s. For all M , M-PSMA achieves greater energy efficiency than M-ALOHA. Additionally, M-PSMA remains efficient at high offered loads, whereas the efficiency of M-ALOHA approaches 0% at high offered load for all M . Again, performance reaches a limit around $M = 4$ for M-PSMA and $M = 8$ for M-ALOHA. Fig. 9(b)

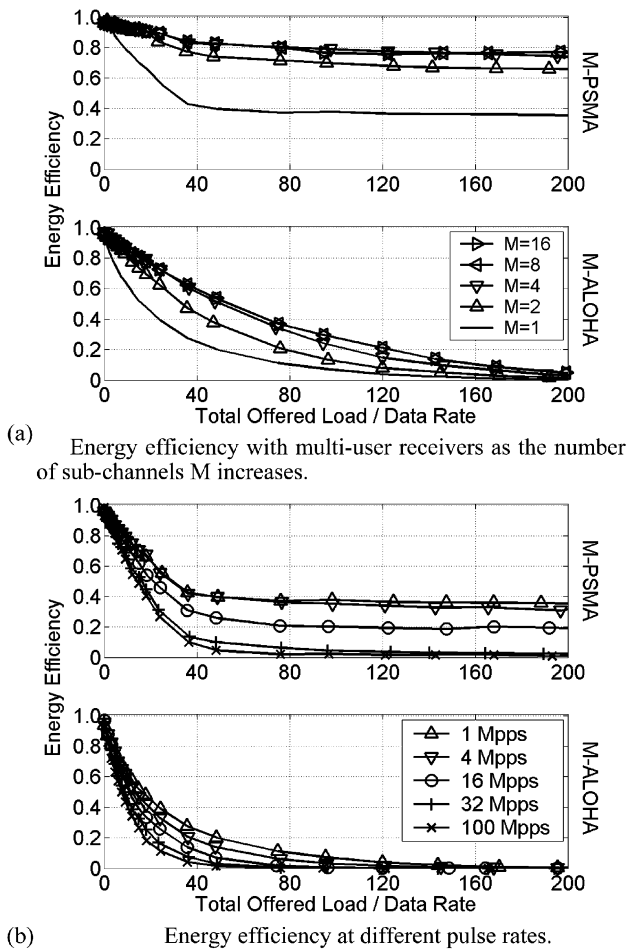


Fig. 9. Energy efficiency for M-PSMA and M-ALOHA.

shows that the energy efficiency decreases as the pulse rate increases because the reduced number of time slots cause more collisions. For M-PSMA, the energy efficiency starts to decrease rapidly around 16 Mp/s and reaches a floor by 32 Mp/s. The efficiency of M-ALOHA transitions more gradually, but it also reaches a floor around 32 Mp/s.

Next, we compare the performance of BSMA, M-PSMA, and M-ALOHA to a baseline distributed PSMA/CA protocol and to a baseline centralized TDMA protocol. Note that the proposed techniques in Section IV keep the performance of BSMA roughly independent of pulse rate³ so we simulate at 1 Mp/s for a fair comparison among protocols. The number of sub-channels is $M = 1$, except for TDMA, which has $M = 8$ time slots. For TDMA, an omniscient central controller perfectly schedules time slots for exclusive channel access and spatial multiplexing. In an actual *ad hoc* network, the centralized control and single point of failure for TDMA is undesirable.

Fig. 10(a) shows that M-PSMA attains an even higher throughput than centralized TDMA with perfect scheduling. M-PSMA outperforms TDMA, BSMA, and PSMA/CA because it allows sub-channel interleaving; and it outperforms M-ALOHA because it checks for a busy medium before transmitting. The random scheduling of BSMA achieves a throughput

³The 2-ns switching time required by (6) does limit the performance of BSMA, but only for PRIs well below our moderate range. A full switching cycle limits the maximum pulse rate to $250 \text{ Mp/s} = 1 \text{ pulse}/(2 \times 2 \text{ ns})$

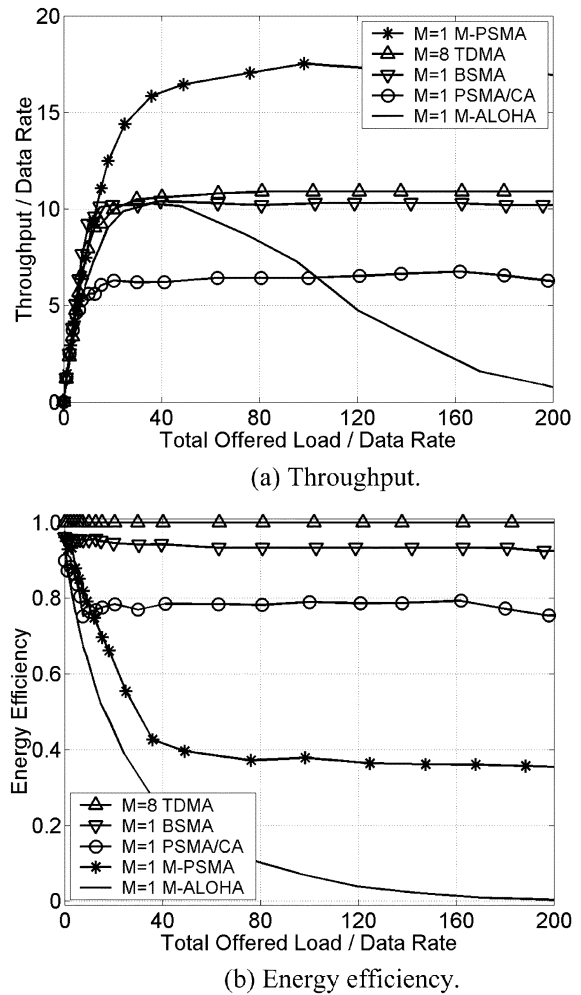


Fig. 10. Performance comparison of M-PSMA, PSMA/CA, M-ALOHA, BSMA, and TDMA [24].

close to the perfect scheduling of TDMA. BSMA avoids most collisions, and it efficiently handles collisions when they do occur. BSMA outperforms PSMA/CA because the handshaking packets add overhead. Further, BSMA allows transmissions under exposed node conditions, whereas PSMA/CA does not. M-ALOHA performs worse than even PSMA/CA at high offered loads because the lack of virtual CCA or a pulse sensor results in a considerable number of collisions.

Fig. 10(b) compares the energy efficiency of M-PSMA, M-ALOHA, and BSMA to PSMA/CA and TDMA at 1 Mp/s. From the perspective of energy efficiency, the protocols rank much differently than from the perspective of throughput. BSMA is the most energy efficient distributed protocol, and it performs nearly as well as centralized TDMA. BSMA outperforms PSMA/CA because the RTS packets may directly collide with data packets or indirectly cause collisions by interfering with control packets. BSMA outperforms M-ALOHA and M-PSMA because neither multichannel protocol has a mechanism to detect or avoid collisions. At low offered load, the energy efficiency of M-PSMA follows that of PSMA/CA. At high offered load, M-PSMA attains about half the energy efficiency of PSMA/CA, but it outperforms M-ALOHA because it checks for channel activity before transmitting. Under

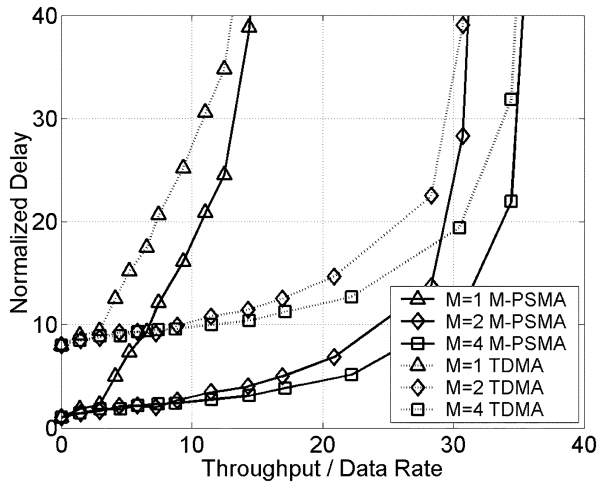


Fig. 11. Normalized delay for M-PSMA and TDMA [24].

M-ALOHA, most transmissions collide with each other at high offered load, and the energy efficiency approaches 0%. In Fig. 10, M-ALOHA and M-PSMA operate under single-user receivers so they may drop some transmissions due to a busy receiver. Note, however, that increasing M to $M = 16$ still does not improve the energy efficiency of M-ALOHA or M-PSMA to that of BSMA.

Ignoring the relatively small propagation time, the average transmission delay D of a packet is [22], [41]

$$D = \left(\frac{G}{S} - 1 \right) \times (N + \delta) + N \quad (10)$$

where G is the offered load, S is the throughput at G , $1/N$ is a sub-channel's proportion of total link bandwidth, δ is the average retransmission delay computed from the simulations, and $N + \delta$ is the normalized average delay between successive retransmissions. We compare the delay of a 1-Mp/s M-PSMA system to a hypothetical 1-Mp/s TDMA system that can achieve the same throughput at each M . We show M-PSMA only because it outperforms M-ALOHA, and BSMA has no advantage in delay over TDMA. Fig. 11 plots the M-PSMA delay with solid lines and the TDMA delay with dotted lines. TDMA incurs a much longer delay than M-PSMA for low offered load (i.e., when G/S is close to 1). This is because each sub-channel's bandwidth decreases by a factor of N so it takes N times longer to transmit a packet on an empty channel. For the proposed M-PSMA MAC, N is always one because each successful transmission uses the full channel bandwidth.

VI. CONCLUSION

I-UWB is an attractive radio technology for *ad hoc* and sensor networks due to its robustness to multipath fading, sub-centimeter ranging ability, and low-cost low-power hardware. We have proposed three distributed MAC protocols that are custom tailored to large *ad hoc* and sensor networks with I-UWB radios. None of the protocols significantly complicates hardware, adds control traffic overhead, or has a central point of failure. The proposed protocols outperform more general approaches such as CA or time division.

The two multichannel MAC protocols, i.e., M-PSMA and M-ALOHA, can significantly reduce the probability of collision, depending on the PRI and the channel conditions. In contrast to traditional multichannel MACs and handshaking schemes, M-PSMA and M-ALOHA improve performance without reducing link bandwidth, increasing delay, adding hardware complexity, or adding handshaking overhead. In terms of throughput and delay, M-PSMA outperforms all other protocols, and it is suitable for distributed networks that require a high aggregate throughput. A multiuser I-UWB receiver, which can receive several time-interleaved transmissions concurrently, further improves throughput, and it brings the energy efficiency of M-PSMA close to that of PSMA/CA.

The busy-signal protocol, i.e., BSMA, provides superior energy efficiency over other distributed MAC protocols because source nodes can assess the status of ongoing data transmissions. Hence, BSMA is a suitable protocol for energy-sensitive networks. Whereas narrowband systems require two transceivers to implement a busy-signal MAC protocol, our I-UWB system requires only one transceiver to save cost, power, and circuit complexity. Simulations show that our physical layer design techniques result in a busy signal that is easily detectable and that does not interfere with data reception.

REFERENCES

- [1] S. Verdú, "Spectral efficiency in the wideband regime," *IEEE Trans. Inf. Theory*, vol. 48, no. 6, pp. 1319–1343, Jun. 2002.
- [2] L. W. Fullerton, "Reopening the electromagnetic spectrum with ultrawideband radio for aerospace," in *IEEE Proc. Aerosp. Conf.*, Mar. 2000, vol. 11, pp. 201–210.
- [3] M. Nakagawa, H. Zhang, and H. Sato, "Ubiquitous homelinks based on IEEE 1394 and ultra wideband solutions," *IEEE Commun. Mag.*, vol. 41, no. 4, pp. 74–82, Apr. 2003.
- [4] D. G. Leeper, "A long-term view of short-range wireless," *Comput.*, vol. 34, no. 6, pp. 39–44, Jun. 2001.
- [5] F. Cuomo, C. Martello, A. Baiocchi, and F. Capriotti, "Radio resource sharing for *ad hoc* networking with UWB," *IEEE J. Sel. Areas Commun.*, vol. 20, no. 12, pp. 1722–1732, Dec. 2002.
- [6] S. S. Kolenchery, J. K. Townsend, and J. A. Freebersyser, "A novel impulse radio network for tactical military wireless communications," in *IEEE Military Commun. Conf.*, Oct. 1998, vol. 1, pp. 59–65.
- [7] J. Zhang, R. A. Kennedy, and T. D. Abhayapala, "New results on the capacity of m -ary PPM ultra-wideband systems," in *IEEE Int. Commun. Conf.*, May 2003, vol. 4, pp. 2867–2871.
- [8] M. Z. Win and R. A. Scholtz, "Ultra-wide bandwidth time-hopping spread-spectrum impulse radio for wireless multiple-access communications," *IEEE Trans. Commun.*, vol. 48, no. 4, pp. 679–689, Apr. 2000.
- [9] *802.15.3-2003 IEEE Standards for Information Technology—Part 15.3: Wireless Medium Access Control (MAC) and Physical Layer (PHY) Specifications for High Rate Wireless Personal Area Networks (WPAN)*, 802.15.3 Draft Standard, Draft P802.15.3/D17, Feb. 2003.
- [10] J. P. K. Gilb, *Wireless Multimedia: A Guide to the IEEE 802.15.3 Standard*. Piscataway, NJ: IEEE Press, 2004.
- [11] E. Saberinia and A. H. Tewfik, "Multi-user UWB-OFDM communications," in *IEEE Pacific Rim Commun., Comput., Signal Process. Conf.*, Aug. 2003, vol. 1, pp. 127–120.
- [12] G. R. Aiello and G. D. Rogerson, "Ultra-wideband wireless systems," *IEEE Micro*, vol. 4, no. 2, pp. 36–47, Jun. 2003.
- [13] Z. Shiwei, L. Huaping, and S. Mo, "Performance of a multi-band ultra-wideband system over indoor wireless channels," in *1st IEEE Consumer Commun. Networking Conf.*, Jan. 2004, pp. 700–702.
- [14] J. Balakrishnan, A. Batra, and A. Dabak, "A multi-band OFDM system for UWB communication," in *Proc. IEEE Ultra Wideband Syst. Technol. Conf.*, Nov. 2003, pp. 354–358.
- [15] N. Boubaker and K. B. Letaief, "Ultra wideband DSSS for multiple access communications using antipodal signaling," in *IEEE Int. Commun. Conf.*, May 2003, vol. 3, pp. 2197–2201.
- [16] L. Qinghua and L. A. Rusch, "Multiuser detection for DS-SSMA UWB in the home environment," *IEEE J. Sel. Areas Commun.*, vol. 20, no. 12, pp. 1701–1711, Dec. 2002.

- [17] P. Runkle, J. McCorkle, T. Miller, and M. Welborn, "DS-CDMA: The modulation technology of choice for UWB communications," in *Proc. IEEE Ultra Wideband Syst. Technol. Conf.*, Nov. 2003, pp. 364–368.
- [18] W. Horie and Y. Sanada, "Novel CSMA scheme for DS-UWB *ad hoc* network with variable spreading factor," in *Joint Workshop Int. Ultra Wideband Syst. Conf. Ultra Wideband Syst. Technol.*, May 2004, pp. 361–365.
- [19] A. Woo and D. E. Culler, "A transmission control scheme for media access in sensor networks," in *Proc. Int. Mobile Comput. Networking Conf.*, Jul. 2001, pp. 221–235.
- [20] 802.15.4-2003 *IEEE Standard for Information Technology—Part 15.4: Wireless Medium Access Control (MAC) and Physical Layer (PHY) specifications for Low Rate Wireless Personal Area Networks (LR-WPANS)*, IEEE Standard 802.15.4, 2003.
- [21] Y. Wei, J. Heidemann, and D. Estrin, "An energy-efficient MAC protocol for wireless sensor networks," in *21st Annu. Joint IEEE Comput. Commun. Societies Conf.*, Jun. 2002, vol. 3, pp. 1567–1576.
- [22] A. Nasipuri, J. Zhuang, and S. Das, "A multichannel CSMA MAC protocol for multihop wireless networks," in *IEEE Wireless Commun. Networking Conf.*, Sep. 1999, vol. 3, pp. 1402–1406.
- [23] A. C. V. Gummalla and J. O. Limb, "Design of an access mechanism for a high speed distributed wireless LAN," *IEEE J. Sel. Areas Commun.*, vol. 18, pp. 1740–1750, Sep. 2000.
- [24] N. J. August, W. C. Chung, and D. S. Ha, "Distributed MAC protocols for UWB *ad hoc* and sensor networks," in *IEEE Radio Wireless Symp.*, Jan. 2006, pp. 511–514.
- [25] "FCC revision of part 15 of the Commission's rules regarding ultra-wideband transmission systems: First report and order," FCC, Washington, DC, Tech. Rep., Feb. 2002. [Online]. Available: http://hraunfoss.fcc.gov/edocs_public/attachmatch/FCC-02-48A1.pdf
- [26] S. Jose, H. J. Lee, D. S. Ha, and S. S. Choi, "A low power CMOS power amplifier for ultra wideband (UWB) applications," in *Int. Circuits Syst. Symp.*, May 2005, pp. 5111–5114.
- [27] R. Thirugnanam, D. S. Ha, and S. S. Choi, "4-bit 1.4 GS/s low power folding ADC for UWB systems," in *IEEE Int. Ultra Wideband Conf.*, Sep. 2005, pp. 536–541.
- [28] S. Wang, D. S. Ha, and S. S. Choi, "A 6-bit 5.4-Gsamples/s CMOS D/A converter for DS-CDMA UWB transceivers," in *IEEE Int. Ultra Wideband Conf.*, Sep. 2005, pp. 333–338.
- [29] K. Marsden, H.-J. Lee, D. S. Ha, and H.-S. Lee, "Low power CMOS re-programmable pulse generator for UWB systems," in *IEEE Ultra Wideband Syst. Technol. Conf.*, Nov. 2003, pp. 443–337.
- [30] N. J. August, H. J. Lee, and D. S. Ha, "Design of pulse sensor to detect medium activity in UWB networks," in *IEEE Int. Ultra Wideband Conf.*, Sep. 2005, pp. 70–75.
- [31] H. J. Lee, D. S. Ha, and H.-S. Lee, "Toward digital UWB radios: Part II—A system design to increase data throughput for a frequency domain UWB receiver," in *Joint Int. Workshop Ultra Wideband Syst. Conf. Ultra Wideband Syst. Technol.*, May 2004, pp. 253–257.
- [32] H. Lee and D. Ha, "A frequency domain approach for all-digital CMOS ultra wideband receivers," in *IEEE Ultra Wideband Syst. Technol. Conf.*, Nov. 2003, pp. 86–90.
- [33] H.-J. Lee, D. S. Ha, and H.-S. Lee, "Toward digital UWB radios: Part I—Frequency domain UWB receiver with 1 bit ADCs," in *Proc. Joint Int. Workshop Ultra Wideband Syst. Conf. Ultra Wideband Syst. Technol.*, May 2004, pp. 248–252.
- [34] J.-Y. Le Boudec, R. Merz, B. Radunovic, and J. Widmer, "DCC-MAC: A decentralized MAC protocol for 802.15.4a-like UWB mobile *ad hoc* networks based on dynamic channel coding," in *Proc. 1st Annu. Broadband Networks Conf.*, Oct. 2004, pp. 396–405.
- [35] M.-G. Di Benedetto, L. De Nardis, M. Junk, and G. Giancola, "(UWB)₂: Uncoordinated, wireless, baseborn, medium access control for UWB communication networks," *Mobile Networks Applicat.*, 3rd quarter, 2005, to be published.
- [36] A. El Fawal, J.-Y. Le Boudec, R. Merz, B. Radunovic, J. Widmer, and G. M. Maggio, "Tradeoff analysis of PHY-aware MAC in low-rate, low-power UWB networks," *IEEE Commun. Mag.*, vol. 43, no. 12, pp. 147–155, 2005.
- [37] G. Giancola, C. Martello, F. Cuomo, and M.-G. Di Benedetto, "Radio resource management in infrastructure-based and *ad hoc* UWB networks," *Wireless Commun. Mobile Comput.*, vol. 5, no. 5, pp. 581–597, Aug. 2005.
- [38] J. Ding, L. Zhao, S. Medidi, and K. Sivalingam, "MAC protocols for ultra-wide-band (UWB) wireless networks: Impact and channel acquisition time," in *Proc. SPIE ITCOM02*, Jul. 2002, pp. 97–106.
- [39] J. Foerster, IEEE 802.15 WPANs, "Channel Modeling Subcommittee report (final)," Tech. Rep. P802. 15-02/368r5-SG3a, Dec. 2000. [Online]. Available: http://grouptrt.ieee.org/groups/802/15/pub/2002/Nov02/02490r0P802-15_SG3a-Channel-Modeling-Subcommittee-Report-Final.zip.
- [40] F. Xue and P. R. Kumar, "The number of neighbors needed for connectivity of wireless networks," *ACM Wireless Networks*, vol. 10, no. 2, pp. 169–181, Mar. 2004.
- [41] N. J. August, H.-J. Lee, and D. S. Ha, "An efficient multi-user UWB receiver for distributed medium access in *ad hoc* and sensor networks," in *IEEE Radio Wireless Conf.*, Sep. 2004, pp. 455–458.
- [42] F. Tobagi and L. Kleinrock, "Packet switching in radio channels: Part II—The hidden terminal problem in carrier sense multiple-access and the busy-tone solution," *IEEE Trans. Commun.*, vol. COMM-23, no. 12, pp. 1417–1433, Dec. 1975.
- [43] C. Wu and V. Li, "Receiver-initiated busy-tone multiple access in packet radio networks," in *Proc. ACM Frontiers Comput. Commun. Technol. Workshop*, Stowe, VT, Aug. 11–13, 1987, pp. 336–342.
- [44] L. W. Fullerton, "Full duplex ultrawide-band communication system and method," U.S. Patent 5 687 169, Nov. 11, 1997.
- [45] N. J. August and D. S. Ha, "An efficient UWB radio architecture for busy signal MAC protocols," in *IEEE Sensor and Ad Hoc Commun. Networks Conf.*, Oct. 2004, pp. 10–10.



Nathaniel J. August (S'03–M'05) was born in Cumberland, MD, in 1975. He received the B.S. degree in computer engineering (with a minor in computer science), M.S. degree in electrical engineering, and Ph.D. degree in electrical engineering from the Virginia Polytechnic Institute and State University, Blacksburg, in 1998, 2001, and 2005, respectively.

From 1995 to 2005, during internships, he was a Validation Engineer with the Intel Corporation in both their Folsom, CA and Portland, OR branches.

In April 2006, he joined the Intel Corporation in Portland, OR, as a Component Design Engineer. He has authored ten papers in the field of UWB communication. He coauthored *An Introduction to Ultra Wideband Communication Systems* (Prentice-Hall, 2005). His research interests include low-power very large scale integration (VLSI) design, video codecs, signal processing, RF identification (RFID) systems, and UWB communications systems.



Dong Sam Ha (M'86–SM'97) received the B.S. degree in electrical engineering from Seoul National University, Seoul, Korea, in 1974, and the M.S. and Ph.D. degrees in electrical and computer engineering from the University of Iowa, Iowa City, in 1984 and 1986, respectively.

Since Fall 1986, he has been a faculty member with the Department of Electrical and Computer Engineering, Virginia Polytechnic Institute (Virginia Tech) and State University, Blacksburg. He is currently a Professor and Director of the Center for

Embedded Systems and Critical Applications (CESCA). He supervises the Virginia Tech VLSI for Telecommunications (VTVT) Group, which specializes in VLSI design for wireless communications including UWB and wireless sensor systems for monitoring and diagnosis of buildings and vehicles. During a research leave from January to June 2003, he was with Freescale (formerly Xtreme Spectrum), where he was involved in UWB system design and low-power baseband signal processing. Along with his students, he has developed four computer-aided design (CAD) tools for digital circuit testing and has created a standard library of CMOS cells. The library cells and source code for the four tools have been distributed to over 250 universities and research institutions worldwide. He has authored or coauthored 30 papers in the UWB area over the past three years. He contributed to *An Introduction to Ultra Wideband Communication Systems* (Prentice-Hall, 2005). His research interests include low-power VLSI design for wireless communications, low-power/high-speed analog and mixed-signal design, RF integrated-circuit (IC) design, UWB RFIDs, wireless sensor systems for monitoring and diagnosis of buildings and vehicles, and reconfigurable architectures.

Dr. Ha was the general chair of the 2005 System-on-Chip (SOC) Conference and a member of the 2005 Technical Program Committee of the International Conference on Ultra Wideband (ICU).